

Bright Source of Cold Ions for Surface-Electrode Traps

Marko Cetina,¹ Andrew Grier,¹ Jonathan Campbell,² Isaac Chuang,¹ and Vladan Vuletić¹

¹*Department of Physics, MIT-Harvard Center for Ultracold Atoms, and Research Laboratory of Electronics, Massachusetts Institute of Technology, Cambridge, Massachusetts 02139, USA*

²*Department of Physics, United States Military Academy, West Point, NY, 10996*

(Dated: August 15, 2018)

We produce large numbers of low-energy ions by photoionization of laser-cooled atoms inside a surface-electrode-based Paul trap. The isotope-selective trap loading rate of 4×10^5 Yb⁺ ions/s exceeds that attained by photoionization (electron impact ionization) of an atomic beam by four (six) orders of magnitude. Traps as shallow as 0.13 eV are easily loaded with this technique. The ions are confined in the same spatial region as the laser-cooled atoms, which will allow the experimental investigation of interactions between cold ions and cold atoms or Bose-Einstein condensates.

PACS numbers: 42.50.Dv, 03.67.Hk, 42.50.Gy, 32.80.Pj

Among many candidate systems for large-scale quantum information processing, trapped ions currently offer unmatched coherence and control properties [1]. The basic building blocks of a processor, such as quantum gates [2], subspaces with reduced decoherence [3], quantum teleportation [4, 5], and entanglement of up to eight ions [6, 7] have already been demonstrated. Nevertheless, since a logical qubit will likely have to be encoded simultaneously in several ions for error correction [8, 9], even a few-qubit system will require substantially more complex trap structures than currently in use. Versatile trapping geometries can be realized with surface-electrode Paul traps, where electrodes residing on a surface create three-dimensional confining potentials above it [10]. In contrast to three-dimensional traps [11, 12, 13], such surface traps can be patterned using standard lithographic techniques, and allow increased optical access to the ions and real-time control over their position in all directions.

While the prospect of scalable quantum computing has been the main motivation for developing surface-electrode traps, it is likely that this emerging technology will have a number of other important, and perhaps more immediate, applications. Porras and Cirac have proposed using dense lattices of ion traps, where neighboring ions interact via the Coulomb force, for quantum simulation [14]. A lattice, with a larger period to avoid ion-ion interactions altogether, could allow the parallel operation of many single-ion optical clocks [15], thereby significantly boosting the signal-to-noise ratio. The increased optical access provided by planar traps could be used to couple a linear array of ion traps to an optical resonator and efficiently map the stored quantum information onto photons [16]. Since the surface-electrode arrangement allows one to move the trap minimum freely in all directions, ions can be easily embedded in an ensemble of cold neutral atoms for investigations of cold ion-atom collisions [17], charge transport [18], or even the interaction of a single ion with a Bose-Einstein condensate [19].

Compared to standard Paul traps [11, 12, 13], the open geometry of surface-electrode traps restricts the

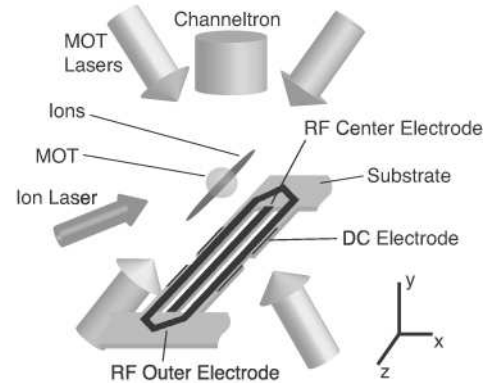


Figure 1: Setup for loading a surface-electrode ion trap by in-trap photoionization of laser-cooled atoms. A ^{172}Yb or ^{174}Yb magneto-optical trap (MOT) is formed 4 mm above the trap surface. Cold Yb⁺ ions are produced inside the Paul trap by single-photon excitation from the excited 1P_1 atomic state.

trap depth and increases the susceptibility to stray electric fields, making trap loading and compensation more difficult. Nevertheless, successful loading from a thermal atomic beam has recently been demonstrated using photoionization [20] or electron-impact ionization aided by buffer gas cooling [21]. The former [22, 23] is superior in that it provides faster, isotope-selective loading [20, 24, 25, 26]. However, the loading rate and efficiency remain relatively low, and charge exchange collisions make it difficult to load pure samples of rare isotopes [25].

In this Letter, we demonstrate that large numbers of low-energy ions can be produced by photoionization of a laser-cooled, isotopically pure atomic sample, providing a robust and virtually fail-safe technique to load shallow or initially poorly compensated surface ion traps. We achieve a loading rate of 4×10^5 Yb ions per second into a $U_0 = 0.4$ eV deep printed-circuit ion trap, several orders of magnitude larger than with any other method demonstrated so far, and have directly loaded traps as

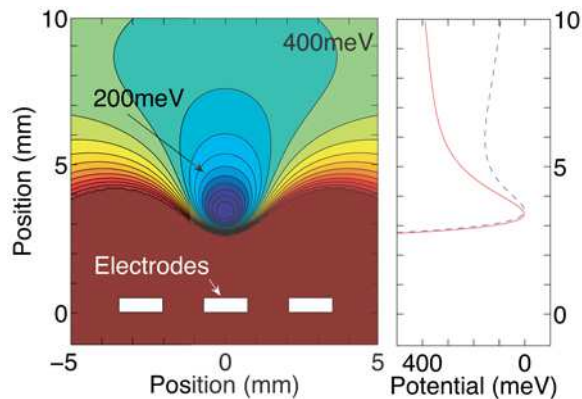


Figure 2: Left: Trapping pseudopotential for RF amplitudes of $V_o = 560$ V and $V_c = -340$ V applied to the outer and center electrodes together with a DC bias of -1.25 V applied to all electrodes. The contours are spaced by 50 meV. Right: The dc-unbiased trap (dashed blue curve) exhibits less micromotion heating but is significantly shallower than the dc-biased trap (solid red curve). (Color Online)

shallow as $U_0 = 0.13$ eV. The trapping efficiency for the generated low-energy ions is of order unity. We also realize the first system where ions are confined in the same spatial region as laser-cooled atoms, allowing for future experimental studies of cold ion-atom collisions.

Efficient photoionization of Yb atoms is accomplished with a single photon from the excited 1P_1 state that is populated during laser cooling, and that lies 3.11 eV, corresponding to a 394 nm photon, below the ionization continuum. Due to momentum and energy conservation, most of the ionization photon's excess energy is transferred to the electron. Therefore, when we ionize atoms at rest even with 3.36 eV (369 nm) photons – the ion cooling light – the calculated kinetic energy of the ions amounts to only 8 mK (0.7 μ eV). Every ion generated inside the trap should therefore be captured, and we easily observe ion trapping even without subsequent laser cooling.

The ion trap is a commercial printed circuit on a vacuum-compatible substrate (Rogers 4350) with low radiofrequency (RF) loss. The three 1 mm-wide, 17.5 μ m-thick copper RF electrodes are spaced by 1 mm wide slits (Fig.1), whose inner surfaces are metallized to avoid charge buildup on dielectric surfaces. The two outer RF electrodes are electrically connected. Twelve dc electrodes placed outside the RF electrodes provide trapping in the axial direction, and permit cancellation of stray electric fields. In addition, the RF electrodes can be dc-biased to apply a vertical electric field. All dielectric surfaces outside the dc electrodes have been removed with the exception of a 500 μ m strip supporting the dc electrodes.

The ratio between the RF voltages V_c (applied to the center electrode) and V_o (outer electrode) determines the

trap height above the surface. With a typical value of $V_c/V_o = -0.63$, the RF node is located 3.6(1) mm above from the surface. For $V_o = 540$ V applied to the outer electrodes, at an RF frequency of 850 kHz the secular trap potential has a predicted depth of $U_0 = 0.16$ eV (Fig.2) and a measured secular frequency of 60 kHz. The trap can be deepened by applying a static negative bias voltage V_{dc} to all RF electrodes [21], Fig.2, and unbiased once the ions are loaded. Using $V_{dc} = 0.5$ V we were able to load traps at RF voltages as low as $V_o = 250$ V, corresponding to $U_0 = 0.13$ eV.

All Yb and Yb^+ cooling, detection and photoionization light is derived from near-UV external-cavity diode lasers. ^{172}Yb or ^{174}Yb atoms are laser-cooled in a magneto-optical trap (MOT) using the $^1S_0 \rightarrow ^1P_1$ transition at 399 nm [27]. A master-slave laser system consisting of an external-cavity grating laser and an injected slave laser using violet laser diodes (Nichia Corp. NDHV310ACAE1) delivers 10 mW in three pairs of 1.7 mm beams. The MOT, located 4 mm above the substrate, is loaded from an atomic beam produced by a resistively heated oven placed 8 cm from the trapping region. Typically 5×10^5 Yb atoms are loaded into the MOT with a lifetime of 300 ms at an estimated temperature of a few mK.

Photoionization from the excited 1P_1 state populated during laser cooling is accomplished using either the ion cooling laser at 370 nm with a power of 750 μ W and intensity of 850 mW/cm², or a focused UV light-emitting diode (UV LED, Nichia Corp. NCCU001, emission at (385 ± 10) nm) with a power of 8.7 mW and intensity of 125 mW/cm² at the MOT position. The efficiency of ionization is manifest as a 30% decrease in MOT atom number due to an increase in the MOT decay rate constant by $\Gamma = 0.3$ s⁻¹. The generated ions are also detected directly with a Burle Magnum 5901 Channeltron avalanche detector located 4 cm above the MOT. The UV-light induced MOT loss depends linearly on UV laser intensity (Fig.3), indicating that the ionization process involves a single 370 nm photon. We have also confirmed that the dominant ionization proceeds from the 1P_1 state: when we apply on/off modulation to both the 399 nm MOT light and the 370 nm UV light out of phase, such that the UV light interacts only with ground-state atoms, we observe more than 13-fold decrease in ionization compared to in-phase modulation. From the observed loss rate in combination with an estimated saturation $s = 0.6 - 2$ of the $^1S_0 \rightarrow ^1P_1$ MOT transition, we determine a cross section $\sigma = 4 \times 10^{-18}$ cm² for ionization of ^{174}Yb with 370 nm light from the excited 1P_1 state. We estimate that this value is accurate to a factor of two, due to uncertainties in the 1P_1 population.

The photoionization typically produces 4×10^5 cold ions per second near the minimum of the pseudopotential. Trapped-ion detection with the Channeltron provides rapid readout, making it particularly useful for ob-

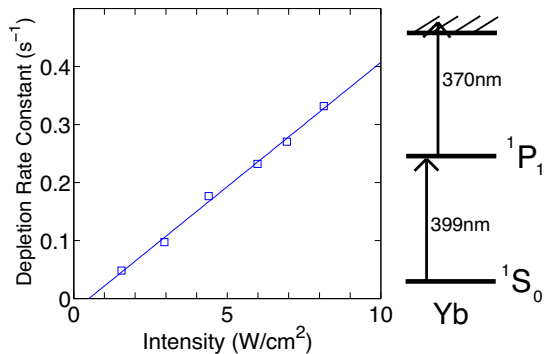


Figure 3: Linear dependence of the loss rate constant of a ^{174}Yb MOT (rms width of $300\text{ }\mu\text{m}$) on 370 nm beam peak intensity ($w = 43\text{ }\mu\text{m}$), indicating that photoionization is accomplished with a single 370 nm photon from the 1P_1 state that is populated during laser cooling with 399 nm light.

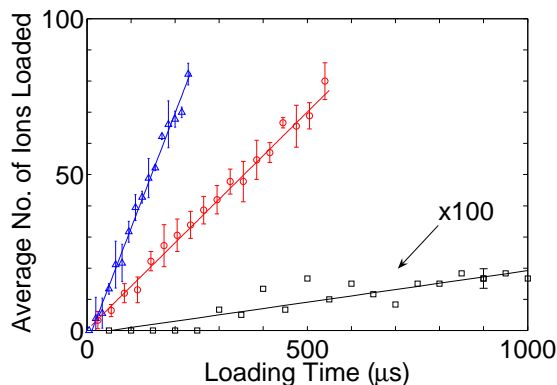


Figure 4: Number of trapped ^{172}Yb ions for photoionization loading with the UV LED from an atomic beam (black squares), from a MOT (red circles), and from a MOT with additional 370 nm laser light (blue triangles). The fitted rates are 2.0×10^2 , 1.4×10^5 , and 3.8×10^5 ions/s, respectively. (Color online)

serving fast trap loading or searching for an initial signal with a poorly compensated trap. Since the detector electric field overwhelms the pseudopotential, we turn on the Channeltron in $1\text{ }\mu\text{s}$ using a Pockels cell driver which is fast compared to the $3.3\text{ }\mu\text{s}$ flight time of the ions. The Channeltron signal is calibrated against fluorescence from a known number of ions, as described below.

We measure ion loading rates by varying the time between turning on the trap and switching on the detector, which empties the trap. Given the brightness of our cold-ion source, ion trapping is easily accomplished even without laser cooling of the ions. Fig.4 shows the loading rate for photoionization of atoms from the MOT and from the atomic beam for the trap potential of depth of $U_0=0.4\text{ eV}$ shown in Figure2. The *loading* rate from the MOT,

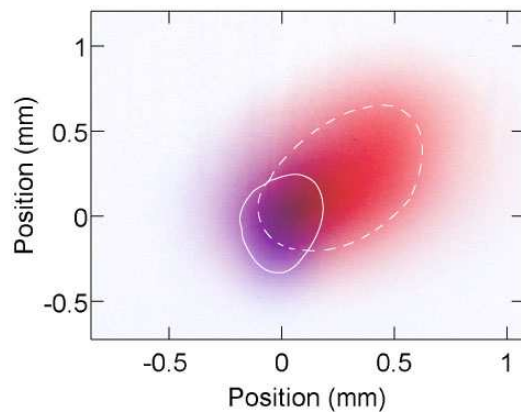


Figure 5: Spatially overlapping ion and atom clouds. The false color image shows a trapped $^{172}\text{Yb}^+$ ensemble containing 10^2 - 10^3 ions (blue cloud lower left), placed inside a magneto-optical trap containing 5×10^5 neutral ^{172}Yb atoms (red cloud upper right). The solid and dashed line indicate the half-maximum contour for the ions and atoms, respectively. (Color online)

4×10^5 ions/s, is three orders of magnitude higher than that from the beam alone, compared to a ratio of only four in the ion *production* rates measured without trap. Thus ions that were produced from laser-cooled atoms in a magneto-optical trap are 200 times more likely to be trapped than ions produced from the atomic beam. We ascribe this difference to the much higher MOT atomic density near the ion-trap minimum and to the lower energy of the produced ions. As the MOT is isotopically pure, our observations of a 10^3 loading rate ratio between MOT and atomic beam imply an additional achievable factor of 10^3 in isotope selectivity beyond the 370:1 isotope selectivity resulting from spectrally selective photoionization in an atomic beam [25].

From comparisons of electron-impact ionization loading and atomic-beam photoionization loading performed by other groups [24, 25], we conclude that our loading rate is six to seven orders of magnitude higher than that achieved with traditional electron-impact ionization and four orders of magnitude higher than all previous results. In addition, by comparing the typical observed loss rate from the MOT (1.1×10^5 atoms/s) to the typical observed loading rate (2.4×10^5 ions/s) under similar conditions, we conclude that our trapping efficiency is comparable to unity. We attribute the discrepancy in rates to calibration of the Channeltron ion detector and uncertainty in the MOT population. This efficiency may prove an important advantage for suppressing anomalous ion heating that has been linked to electrode exposure to the atomic beam during the loading process [13]. The large loading rate will also be beneficial for applications that require a large, isotopically pure sample, such as quantum simulation in an ion lattice [14].

The loaded ions are cooled and observed via fluorescence using an external-cavity grating laser. [28]. To reach the target wavelength of 369.525 nm with a 372 nm laser diode (Nichia) in a Littrow setup with a first-order grating reflectivity of 28%, we cool the diode to temperatures between -10 and -20°C in a moisture-tight container. The laser provides an output power of 1.5 mW and is continuously tunable over more than 10 GHz.

For laser cooling of Yb^+ , the laser is typically tuned 200 MHz below the $^2S_{1/2} \rightarrow ^2P_{1/2}$ transition. An external-cavity repumper laser operating at 935 nm is also necessary to empty the long-lived $^2D_{3/2}$ state on the $^2D_{3/2} \rightarrow ^3D[3/2]_{1/2}$ transition [29]. The UV light scattered by the ions is collected with an aspheric lens of numerical aperture 0.40 placed inside the vacuum chamber at a distance of 19 mm from the trap. The collected light passes through an interference filter, and is evenly split between a charge-coupled device camera and a photomultiplier. The maximum photomultiplier count rate is 5000 s^{-1} per ion. To calibrate the Channeltron detector, we first cool a small cloud of ions (approximately 100) to below the crystallization temperature, as identified by a sudden change in the fluorescence [30]. By comparing the resonance fluorescence of the crystal to that of a single trapped ion, we determine the absolute number of ions loaded, and subsequently measure the Channeltron signal for the same cloud.

The optical observation of the trapped ions allows us to determine the trap position and optimize the overlap with the MOT. We move the MOT laterally using magnetic bias coils and the ion trap vertically by changing the amplitude ratio of the voltages applied to the two RF electrodes. Fig.5 shows that for the optimal loading position of the trap, the pseudopotential minimum is located inside the neutral-atom cloud. We have thus demonstrated the first trapping of cold ions and neutral atoms in the same spatial region, which will allow the experimental investigation of cold ion-atom collisions.

In conclusion, we have realized a novel, simple and robust system to load large numbers of low-energy ions into a versatile planar ion trap. Further trap miniaturization while maintaining a large loading rate can be achieved with a nested electrode design, where large outer electrodes provide initial trapping, and a series of smaller inner electrodes provides stronger confinement as the ions are transported towards the surface. This system provides the means to realize ion lattices for quantum simu-

lation [14], ionic quantum memory with optical readout [16], many-ion optical clocks, or mixed ion-atom systems for the investigation of cold collisions [17] and charge transport [18].

We would like to thank Brendan Shields and Ken Brown for assistance. This work was supported in part by the NSF Center for Ultracold Atoms.

-
- [1] P. Zoller *et al.*, Eur. Phys. J. D **36**, 204 (2005).
 - [2] C. Monroe, D. M. Meekhof, B. E. King, W. M. Itano, and D. J. Wineland, Phys. Rev. Lett. **75**, 4714 (1995).
 - [3] D. Kielpinski *et al.*, Science **291**, 1013 (2001).
 - [4] M. D. Barrett *et al.*, Nature **429**, 737 (2004).
 - [5] M. Riebe *et al.*, Nature **429**, 734 (2004).
 - [6] D. Leibfried *et al.*, Nature **438** (2005).
 - [7] H. Häffner *et al.*, Nature **438**, 643 (2005).
 - [8] P. W. Shor, Phys. Rev. A **52** (1995).
 - [9] A. M. Steane, Phys. Rev. Lett. **77**, 793 (1996).
 - [10] J. Chiaverini *et al.*, Quantum Inf. Comput. **5**, 419 (2005).
 - [11] D. Stick *et al.*, Nature Phys. **2**, 36 (2006).
 - [12] B. DeMarco *et al.*, Quant. Inform. and Comp. (2001).
 - [13] L. Deslauriers, S. Olmschenk, D. Stick, W. K. Hensinger, J. Sterk, and C. Monroe, Phys. Rev. Lett. **97** (2006).
 - [14] D. Porras and J. I. Cirac, Phys. Rev. Lett. **93**, 263602 (2004).
 - [15] W. H. Oskay *et al.*, Phys. Rev. Lett. **97**, 020801 (2006).
 - [16] M. Keller, B. Lange, K. Hayasaka, W. Lange, and H. Walther, Nature **431**, 1075 (2004).
 - [17] R. Côté and A. Dalgarno, Phys. Rev. A **62**, 012709 (2000).
 - [18] R. Côté, Phys. Rev. Lett. **85**, 5316 (2000).
 - [19] R. Côté, V. Kharchenko, and M. Lukin, Phys. Rev. Lett. **89** (2002).
 - [20] S. Seidelin *et al.*, Phys. Rev. Lett. **96**, 253003 (2006).
 - [21] K. R. Brown *et al.*, Phys. Rev. A **75**, 015401 (2007).
 - [22] N. Kjaergaard, L. Hornekaer, A. M. Thommesen, Z. Videsen, and M. Drewsen, Applied Physics B **71** (2000).
 - [23] S. Gulde *et al.*, **73**, 861 (2001).
 - [24] C. Balzer *et al.*, Phys. Rev. A **73**, 041407(R) (2006).
 - [25] D. M. Lucas, *et al.* Phys. Rev. A **69**, 012711 (2004).
 - [26] M. Keller, B. Lange, and K. Hayasaka, **36**, 613 (2003).
 - [27] C. Y. Park and T. H. Yoon, Phys. Rev. A **68**, 055401 (2003).
 - [28] D. Kielpinski, M. Cetina, J. A. Cox, and F. X. Kärtner, Optics Letters **31** (2005).
 - [29] A. S. Bell, P. Gill, H. A. Klein, A. P. Levick, C. Tamm, and D. Schnier, Phys. Rev. A **44** (1991).
 - [30] F. Diedrich, E. Peik, J. Chen, W. Quint, and H. Walther, Phys. Rev. Lett. **59** (1987).